Macromolecules

Article

pubs.acs.org/Macromolecules

PEE–PEO Block Copolymer Exchange Rate between Mixed Micelles Is Detergent and Temperature Activated

Allen B. Schantz,[†] Patrick O. Saboe,[†] Ian T. Sines,[†] Hee-Young Lee,[†] Kyle J. M. Bishop,[†] Janna K. Maranas,[†] Paul D. Butler,*[,‡,§] and Manish Kumar*[,†]

[†]Department of Chemical Engineering, The Pennsylvania State University, University Park, Pennsylvania 16802, United States

[‡]NIST Center for Neutron Research, National Institute of Standards and Technology, Gaithersburg, Maryland 20899-6102, United States

[§]Department of Chemistry, University of Tennessee, Knoxville, Knoxville, Tennessee 37996-1600, United States

Supporting Information

ABSTRACT: We examine the kinetics of polymer chain exchange between mixed block copolymer–detergent micelles, a system relevant to the synthesis of protein-containing biomimetic membranes. While chain exchange between block copolymer (BCP) aggregates in water is too slow to observe, and detergent molecules exchange between micelles on a time scale of nanoseconds to microseconds, BCP chains exchange between mixed detergent–polymer micelles on intermediate time scales of many minutes to a few days. We examine a membrane-protein-relevant, vesicle-forming, ultrashort polymer, poly(ethyl ethylene)$_{20}$-poly(ethylene oxide)$_{18}$ (PEE$_{20}$–PEO$_{18}$). PEE$_{20}$–PEO$_{18}$ was solubilized in mixed micelles with the membrane protein compatible nonionic detergent octyl-β-D-glucoside (OG). Using cryo-TEM and small-angle neutron scattering (SANS), we demonstrate complete solubilization of the polymer into micelles. Using time-resolved SANS (TR-SANS), we provide the first direct evidence that detergents activate BCP chain exchange and determine kinetic parameters at two detergent concentrations slightly above the critical micellar concentration (CMC) of OG. We find that chain exchange increases 2 orders of magnitude when temperature increases from 35 to 55 °C and that even a 1 mg/mL increase in OG concentration leads to a noticeable increase in exchange rate. Our kinetic data are consistent with a single rate-limiting process rather than the distribution of exchange rates known to exist for BCPs in the absence of detergent, indicating a different exchange mechanism than the simple chain escape dominant in single-component micelles. Using the Arrhenius equation, we determine that at the detergent concentrations examined the activation energy for polymer chain exchange is only 2–3 times higher for PEE$_{20}$PEO$_{18}$ than for short-chained lipids and that the activation barrier decreases with increasing OG concentration. On the basis of these results, we postulate that mixed micelles exchange BCPs through a detergent-mediated process such as the fusion and fragmentation mechanisms also known to occur in micellar systems. These findings explain the need for high detergent concentration and/or temperature to synthesize polymer/protein membranes. Further, we postulate this is a more general phenomenon applicable to mixed micelle systems containing amphiphiles with vastly different solubilities and CMCs differing by many orders of magnitude.

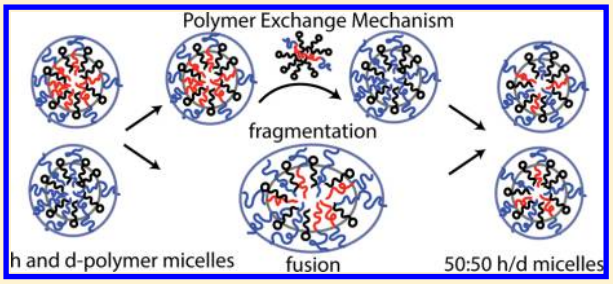

INTRODUCTION

Block copolymers (BCPs) are used for synthesis and assembly of robust biomimetic membranes for proposed applications in drug delivery,[1] DNA sequencing,[2] separations,[3] and sensors.[4−6] BCPs used in biomimetic membranes are amphiphilic and self-assemble into lipid-bilayer-like structures mimicking biological membranes. These membranes can be functionalized by inserting membrane proteins with sophisticated transport[7,8] and sensing mechanisms.[9] Membrane proteins exist within a lipid bilayer *in vivo* and are isolated from cell membranes and stabilized in detergent micelles, which in most cases are composed of nonionic detergents, for structural and functional characterization.[10] Detergent-solubilized membrane proteins have increasingly been combined with ultrashort chained diblock and triblock copolymers (hydrophobic block lengths <110 monomers for a triblock),[8] to form stable self-assembled composite block copolymer–protein membranes.[8,11−19] The major advantages of BCPs over lipids are superior physical[20] and chemical stability,[21] allowing for long-lived BCP nanostructures such as vesicles,[22] micelles,[23] and nanodiscs.[24]

Functionalization of BCP materials by membrane proteins usually requires the presence of detergent to destabilize the BCP aggregates and enable protein insertion. Membrane proteins have been shown to insert into BCP membranes with hydrophobic block length varying by a factor of 5,[8,15] and therefore thicknesses varying by approximately a factor of 2–

Received: September 8, 2016
Revised: March 1, 2017
Published: March 10, 2017

DOI: 10.1021/acs.macromol.6b01973
Macromolecules 2017, 50, 2484–2494

3,[22] while remaining functional. Methods to incorporate proteins in block copolymers include film rehydration[25] and disruption of existing BCP membranes by detergent.[15] These methods have advanced the study of membrane proteins in BCP vesicles but are currently difficult to use to assemble membranes with a high density of proteins. One of the most promising methods to insert a large numbers of membrane proteins is through detergent dialysis, in which both BCPs and membrane proteins are first completely solubilized in detergent micelles and then mixed to form ternary micelles. As these ternary micelles form, the detergent is gradually and selectively removed (based on solubility and size) through a dialysis membrane. This process forms a membrane with the highest packing density of proteins and may result in two-dimensional crystals.[26] To form densely packed membranes via detergent dialysis, block copolymers must associate with protein−detergent micelles, forming ternary micelles that can become BCP−protein membranes once the detergent is removed. Therefore, BCP chain exchange between micelles is an important process in forming protein−BCP membranes.

To date, there have been a number of studies that use detergents to insert membrane proteins into BCPs.[8,11−19] However, there are no direct measurements on the kinetics of block copolymer exchange between mixed BCP/detergent micelles. We can make some inferences about this process based on exchange kinetics observed between other kinds of amphiphile aggregates. The time scale for lipid and cholesterol exchange between vesicles ranges from hours[27,28] to tens of hours for some lipids with longer hydrophobic tails,[29] while detergent micelles can exchange molecules over time scales on the order of nanoseconds[30] to tens of microseconds,[31] and block copolymer aggregates (micelles and vesicles) in water are kinetically frozen.[32,33] In these systems, chain escape from the aggregate is usually a rate-limiting step[27−30,32,34−37] and depends on the balance between the hydrophilic and hydrophobic moiety of the molecule (the lipid tail vs headgroup, BCP hydrophobic block vs hydrophilic block, or detergent hydrophobic chains vs headgroup).[27−29,32,34,35] Because of this dependence on hydrophilic/hydrophobic balance, single-molecule escape for a BCP has a distribution of rates reflecting the polymer's polydispersity index (PDI),[23,38−41] rather than the single rate-limiting process seen in model polymer systems with fixed degrees of polymerization.[42,43] In addition to this single-molecule escape process, detergent[37] and polymer[44] micelles also exchange mass through fission and fusion, although this process is slower than single-molecule escape for most single-component micelles[30,36,44] (an exception being ionic detergents in the presence of a high concentration of counterions[37]).

A number of studies by Rharbi and Winnik have investigated this slower fission/fusion process by examining the exchange of hydrophobic fluorophores between detergent micelles, as these tracer molecules have a lower ability to escape into the aqueous solvent and therefore do not follow the single molecule escape mechanism.[45−48] Exchange in these systems proceeded by two parallel rate-limiting steps: (1) the fusion mechanism, in which two micelles fuse into a large aggregate that quickly splits due to its instability, and (2) the fragmentation mechanism, in which a micelle splits into two parts, one of which is a small micelle containing a tracer molecule. This small micelle quickly grows to full size via fusion and detergent addition. Comparing our system to the detergent/tracer micelles, we can imagine that BCPs might function similarly to the hydrophobic tracer molecules; if they are hydrophobic enough that their escape into the solvent is slower than mixed micelle fragmentation and fusion, then one or more of these processes will become the main method(s) for BCP exchange. Fusion, fragmentation, and single-chain escape exchange mechanisms are depicted in Figure 1.

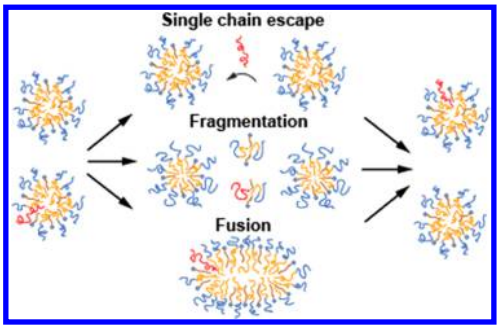

Figure 1. Chain escape, fragmentation, and fusion are three of the possible mechanisms for polymer exchange between mixed micelles. Mixed micelle cores are shown in orange, PEO/detergent headgroup coronas are shown in blue, and the polymer chain that exchanges between the two micelles is red.

In this work, we investigate the transfer of polymer chains between BCP/detergent micelles by means of time-resolved small-angle neutron scattering (TR-SANS). The addition of detergent dramatically increased the chain-exchange rate between otherwise kinetically frozen aggregates, and we were able to model the exchange with a single rate-limiting process, but not with the distribution of rates predicted for pure BCP micelles. We determined the activation energy for the chain exchange process by making measurements at a series of temperatures. Our results provide an understanding of the time scales needed for the initial self-assembly of composite block copolymer/detergent/protein micelles.

MATERIALS AND METHODS

Poly(ethylene oxide)−poly(ethylethylene) (PEE−PEO) synthesis as well as polymer vesicle and micelle preparation are described in detail in the Supporting Information.

Small-Angle Neutron Scattering (SANS). Neutron scattering experiments were conducted using the NGB30 30 m SANS instrument at the NIST Center for Neutron Research (NCNR).[49] Static samples were measured using two different instrument configurations at sample-to-detector distances (SDDs) of 13, 4, and 1 m, with a neutron wavelength of 6 Å and wavelength resolution of $\Delta\lambda/\lambda$ = 14%, while the front end optics were adjusted to optimize the scattering in each Q range. The configurations cover the ranges of $0.003 < Q < 0.04$ Å^{-1}, $0.009 < Q < 0.1$ Å^{-1}, and $0.03 < Q < 0.4$ Å^{-1} and for a complete Q range coverage from $0.003 < Q < 0.4$ Å^{-1}. The scattering vector Q is given by $Q = 4\pi \sin(\theta)/\lambda$, where 2θ is the scattering angle and λ is the neutron wavelength. The scattering from the micelles was greatest in the 4m Q range, so we used that configuration for time-dependent intensity measurements, and the 1m configuration was used to obtain the incoherent background scattering. The full Q range from all three configurations was only used for the static (non-time-dependent) data. All data were collected using NIST demountable cells with quartz windows and nominal thickness 1 mm (see Supporting Information) and corrected for background, transmission, and detector sensitivity and placed on an absolute scale in the usual fashion[49] using NIST's data reduction macros in IGOR Pro.[50] The reduced data were then fit to a monodisperse core−shell model[51] using SasView software.[52]

Time-Resolved SANS (TR-SANS). To determine the kinetics of polymer exchange between micelles, we adopted the general

DOI: 10.1021/acs.macromol.6b01973
Macromolecules 2017, 50, 2484−2494

procedures used in the literature.[23,27,28,32,53,54] In brief, the scattering cross section of noninteracting particles (such as vesicles or micelles in dilute solution) obtained from small-angle neutron scattering is given by eq 1:

$$I(Q) \sim nP(Q)V^2(\rho_{\text{particle}} - \rho_{\text{solvent}})^2 \quad (1)$$

where $I(Q)$ is the scattering intensity, n is the number density of the particles, V is the volume of a single particle, $P(Q)$ is the form factor that depends on the particle's shape, and ρ is the scattering length density (often abbreviated as SLD).[27] Because different isotopes of a single element can have different scattering lengths, isotopic substitution can be used to tune the scattering. In particular, hydrogen and deuterium have very different scattering lengths, and the contrast can therefore be easily manipulated by mixing H_2O and D_2O or by deuteration of molecules in the solute particle.

Thus, in order to observe chain exchange, we mixed two populations of mixed micelles at time 0: one containing partially deuterated polymer with $\rho_{PEE} \approx 1.7 \times 10^{-6}$ Å^{-2} and one containing unsubstituted polymer with $\rho_{PEE} \approx 5 \times 10^{-7}$ Å^{-2}. The micelles are in a solvent containing 79 vol % H_2O and 21 vol % D_2O (corresponding to $\rho \approx 1.1 \times 10^{-6}$ Å^{-2}). The solution also contains some amount of OG detergent, a 5.2% mass fraction of which is tail-deuterated (also corresponding to an average ρ of 1.1×10^{-6} Å^{-2}). The deuteration of the solvent and detergent is such that the average scattering length densities of the mixed h/d solvent and h/d detergent each match that of a polymer micelle core containing a 50:50 mixture of unsubstituted and deuterated PEE (Figure 2). When the polymer exchange goes to

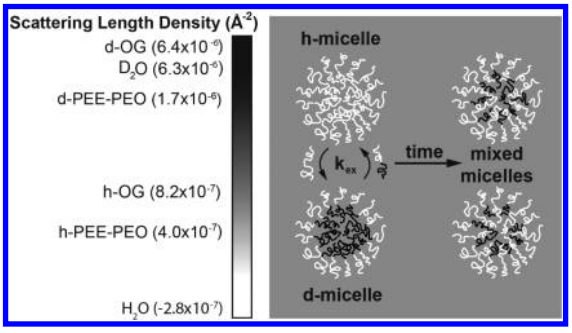

Figure 2. Two populations of micelles, one with d-PEE and one with h-PEE, are mixed at time 0 in a mixture of H_2O/D_2O and d-OG/h-OG contrast-matched to the mixed (equilibrium) micelle core. Because the PEO corona is strongly solvated, most of the scattering is from the micelle core and decays to zero as the chains exchange, so that the micelles become nearly invisible to the neutron beam.[28] OG detergent is present in the micelle but is not shown because the detergent and solvent are contrast-matched from the beginning.

equilibrium, then there should be almost no scattering from the sample above background (see Supporting Information). The micelle corona contains only h-PEO and is therefore not contrast-matched, but is strongly solvated, so that it produces minimal scattering. This scattering, however, is sufficient that prior to mixing the h-polymer micelles scatter more than the d-polymer micelles, but we show in the Supporting Information that this should not affect our kinetic analysis. Therefore, we follow the lead of similar studies[23,40,54] in neglecting corona scattering in determining exchange rates.

At $t = 0$ the scattering intensity as given by eq 1 will be the average of the scattering from the h and d micelle populations. As chain exchange occurs, the contrast between the solvent and micelle core will decrease until at equilibrium the SLD contrast and scattering intensity above background should both be approximately zero. This occurs even though the SLD of each chain is different from that of the solvent because we are observing the system at length scales > 1 nm, so that only the average SLD of the micelle core is important. The extent of chain exchange is therefore simply given by $1 - \Delta\rho(t)/\Delta\rho(0)$ calculated from the scattering intensity using eq 2:

$$\left(\frac{\Delta\rho(t)}{\Delta\rho(0)}\right)^2 = \frac{I(t) - I(\infty)}{I(0) - I(\infty)} \quad (2)$$

where $I(t)$ is the scattering intensity above the incoherent background at time t. We note that eq 2 is independent of Q and thus we make the usual TR-SANS trade of Q (or spatial) resolution for temporal resolution by integrating $I(Q)$ from short (very noisy) runs over a range of Q. In our case $I(t)$ is obtained by integrating $I(Q)$ over the range 0.01 Å^{-1} < Q < 0.046 Å^{-1} after subtracting the incoherent background scattering taken from the high q portion of the data set by averaging over the range 0.12 Å^{-1} < Q < 0.23 Å^{-1}. While technically, as discussed above, the intensity at infinite time, $I(\infty)$, should be about equal to zero; practically, it is very difficult to achieve a perfect contrast match. $I(\infty)$ accounts for any such off-contrast contributions and for scattering from the PEO corona. For a detailed description of this normalization procedure, see the Supporting Information.

All samples were examined until the scattering went to equilibrium or for at least 8 h, with a scan time of 5 min per time point during the first hour and 10 min at longer times. For samples with long exchange times we measured the scattering intensity intermittently for 48 h, keeping the samples at their respective temperatures between measurements. The interval between measurements at long times was on the order of 10 h.

RESULTS

Polymer Aggregate Structure via Cryo-TEM. In the absence of detergent, h-PEE-PEO at 10 mg/mL self-assembles into a mixture of unilamellar vesicles and wormlike structures as shown by Cryo-TEM (Figure 3A). This observation is in agreement with Jain and Bates' 2003 report that a mixture of bilayer and cylinder structures may coexist for PB−PEO over a large range of PB chain length and PEO mass fractions of about 30−50%.[55] Addition of OG detergent solubilizes the large polymer aggregates to form small spherical micelles containing polymer and OG (Figure 3B). We also used dynamic light scattering (DLS) to obtain volume-averaged aggregate size distributions in the presence and absence of OG (see Supporting Information). We observe that in the presence of 7 mg/mL OG or more only aggregates with diameter of order 10 nm are present (corresponding to the small, spherical micelles observed via Cryo-TEM). In the absence of OG, particles with longer diffusion times are present, most likely vesicles and wormlike micelles. Because these large aggregates are absent at the high detergent concentrations used during dialysis (10−40 mg/mL OG[8,15,18]), polymer exchange between them is not relevant to the dialysis process and is not discussed further.

Mixed Micelle Structure from SANS. In order to fully characterize our mixed micelles as a function of temperature and detergent concentration, we fit the SANS data from samples prior to mixing with a monodisperse core−shell sphere form factor[51] using SasView 3.1.1.[52] The solvent SLD, micelle volume fraction, and core SLD of h- or d-PEE were set fixed to their known values, and only the core radius, corona thickness, and corona SLD were varied to obtain the best fit to the data. To mitigate the short collection times used in these kinetic experiments, we further constrained the fits by simultaneously fitting the h- and d-polymer data sets taken at the same conditions of temperature and OG concentration and required that all three fitted parameters (the core radius, corona thickness, and corona SLD) be the same for both cases. This model fits the data well as shown in Figure 4, indicating the contrast and scattering intensity are not sufficient to model with a more sophisticated polymer micelle form factor which would include polymer−polymer interactions in the corona as well as

DOI: 10.1021/acs.macromol.6b01973
Macromolecules 2017, 50, 2484−2494

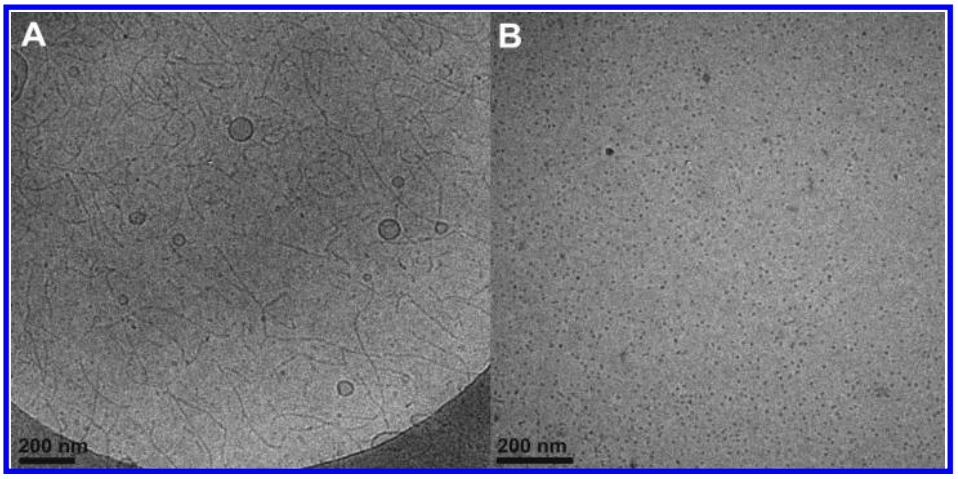

Figure 3. Cryo-TEM was used to probe the overall morphology of the samples used in TR-SANS. (A) PEE_{20}–PEO_{18} self-assembles in water from solvent-evaporated films to form a mixture of wormlike micelles and vesicles. (B) h-PEE–PEO with 7 mg/mL detergent forms small spherical micelles.

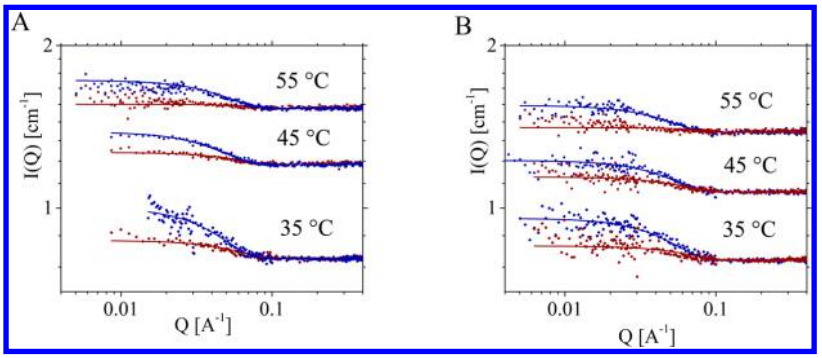

Figure 4. SANS curves and core–shell sphere model fits for the mixed micelles containing 10 mg/mL PEE–PEO and either 7 (A) or 8 (B) mg/mL OG. Blue indicates h-polymer micelles, while red indicates d-polymer. To aid in comparison of h- and d-polymer micelle data, these two static samples used for each kinetic experiment are shifted so that their backgrounds overlap. In addition, the 45 and 55 °C data are shifted upward for clarity, while the 35 °C data are unmodified. Error bars are omitted for clarity, and the scatter in the data is representative of the experimental uncertainty. Scatter in the data depend on collection time and sample–detector distance.

Table 1. Parameters for the Core–Shell Model Fits[a]

T [°C]	[OG] [mg/mL]	r_{core} [Å]	t_{corona} [Å]	$\rho_{corona} \times 10^7$ [Å^{-2}]	h-polymer background [cm^{-1}]	d-polymer background [cm^{-1}]
35	7	41.8 ± 0.5	6.4 ± 0.4	8.0 ± 0.3	0.876	0.806
	8	37.5 ± 0.5	5.3 ± 0.5	7.6 ± 0.3	0.759	0.800
45	7	42.0 ± 0.3	7.7 ± 0.3	8.7 ± 0.1	0.804	0.809
	8	38.8 ± 0.5	5.2 ± 0.5	8.5 ± 0.5	0.871	0.766
55	7	37.3 ± 0.5	4.8 ± 0.5	6.2 ± 0.5	0.929	0.914
	8	37.7 ± 0.5	7.9 ± 0.5	7.7 ± 0.5	0.882	0.869

[a]Note that the solvent SLD is 1.1×10^{-6} Å^{-2} for all samples, and the core SLD is 0.5×10^{-6} Å^{-2} for h-polymer micelles and 1.7×10^{-6} Å^{-2} for d-polymer micelles. Unless stated otherwise, error bars in this paper represent one standard deviation.

a varying SLD across the corona. The model parameters are given in Table 1. We note that the overall micelle radius (core + shell) of ∼4.5 nm obtained from this simplified model is consistent with the 6.5 nm hydrodynamic radius estimated from Stokes' law using DLS (see Supporting Information) and that the micelles are clearly fairly monodisperse, suggesting a thermodynamically equilibrated system. Further it makes clear the source of differing $I(0)$ between the d- and h-polymer is the residual contrast from the highly solvated PEO corona. We note that while often not appreciated this will be true of most of the polymer micelle chain exchange literature.[23,32,33,39–43,53,54,56,57]

Kinetic Analysis. As discussed in the Methods section, the scattering intensity was integrated with respect to Q to obtain a single $\Delta\rho(t)$ for each time point, leading to an intensity decay curve that can be analyzed to obtain the polymer exchange rate. The d- and h-PEE–PEO micelles have higher scattering intensity above background for $Q > 0.1$ Å^{-1} than the premixed (h/d) polymer micelles, which should be very close to the background (Figure 5a). By averaging the scattering intensity of the h- and d-micelles, we obtain the initial scattering intensity of the mixed polymer sample before any exchange has occurred. The premixed sample should have the same scattering intensity as a sample in which the h- and d-polymer chains have been evenly distributed between the micelles through chain

DOI: 10.1021/acs.macromol.6b01973
Macromolecules 2017, 50, 2484–2494

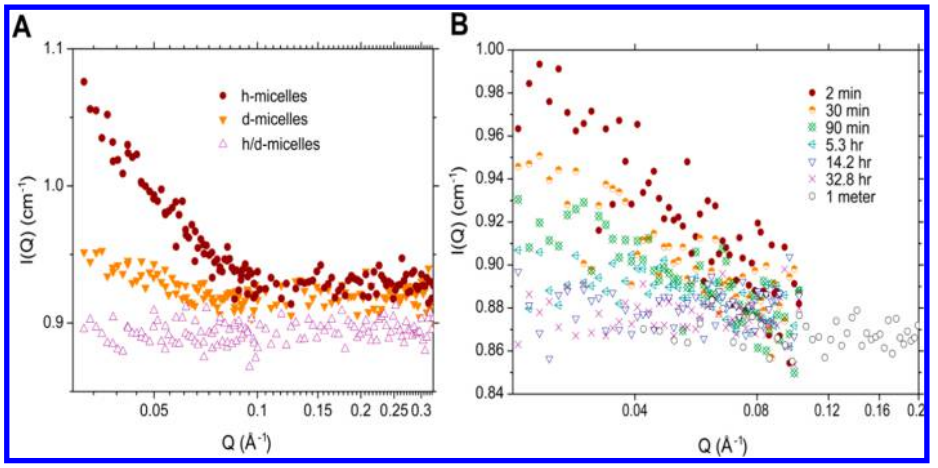

Figure 5. (A) Scattering curves for h- and d-polymer−detergent micelles (top 2 curves) and the premixed h/d-micelles (lower curve). These curves were used to verify the scattering intensity at $t = 0$ and $t = \infty$. This particular sample contains 10 mg/mL PEE−PEO and 7 mg/mL OG at 55 °C. (B) During a kinetic experiment, scattering intensity at the 4 m sample−detector distance decays as h- and d-PEE−PEO distribute between micelles. The intensity at the 1 m sample−detector distance reflects the incoherent background and therefore remains constant. Scattering curves correspond to a sample containing 8 mg/mL OG and 10 mg/mL PEE−PEO at 45 °C. Each sample's background ($0.12\ Å^{-1} < Q < 0.23\ Å^{-1}$) was subtracted from its integrated intensity ($0.01\ Å^{-1} < Q < 0.046\ Å^{-1}$) to find the fractional intensity at each time point (Figure 6), thus trading the unnecessary high spatial resolution with poor statistics for good temporal resolution. Note that the scatter in the data is indicative of the uncertainties, and the error bars have been omitted for clarity.

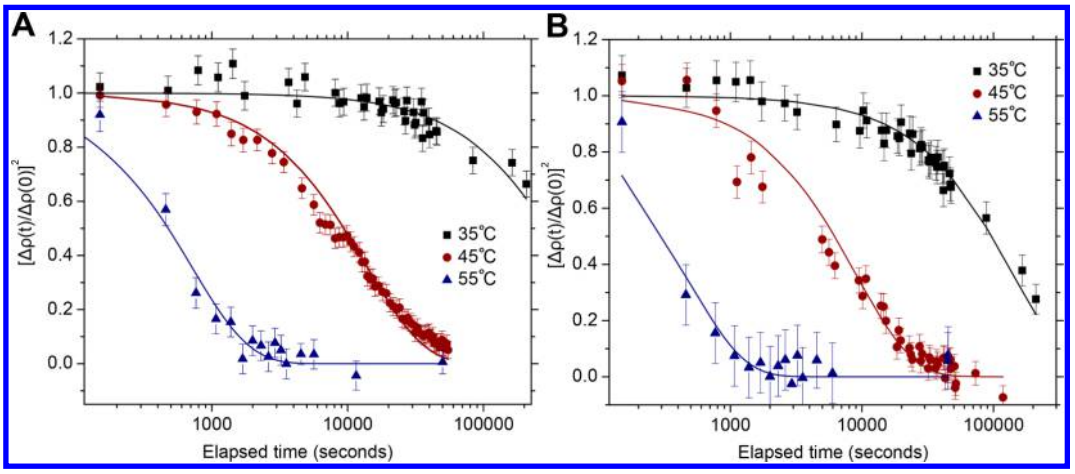

Figure 6. At both 7 mg/mL OG (A) and 8 mg/mL OG (B), increasing temperature dramatically increases the rate of polymer exchange. Blue points represent 55 °C data, red points 45 °C, and black points 35 °C. Lines of the corresponding colors represent the best single-exponential fits to the data. The rate of chain exchange between micelles can also be enhanced by increasing the amount of detergent. Complete chain exchange was achieved at temperatures of 45 °C for 8 mg/mL OG and 55 °C for both OG conditions.

exchange, leading to a minimum of scattering. Figure 5b shows how the scattering intensity decays over time due to polymer exchange, eventually reaching the same value as for the premixed sample.

Because we found that a detergent concentration of at least 7 mg/mL was essential to completely solubilize the polymers into mixed micelles (see Figure 3), we used detergent concentrations of 7−8 mg/mL at three different temperatures (Figure 6) to study the polymer/detergent dynamics. At higher concentration of (invisible) detergent the signal became too weak to reliably process. In the presence of 7 or 8 mg/mL detergent, polymer exchange takes place on a time scale easily observable using TR-SANS (30 min to ∼3 days) at temperatures in the range 35−55 °C.

DISCUSSION

Single-chain escape into the solvent is well-known to be the rate-limiting process for most single-component micelles, particularly BCP micelles, whose hydrophilic coronas create a steric barrier to fusion and fragmentation.[38] Because our mixed micelles are well over 50 mass % BCP, we might expect the PEO corona to remain dense enough that fusion and fragmentation are slower than single BCP escape, and we begin by treating our data in the framework of polymer micelle exchange kinetics. The currently accepted model for polymer exchange by single-chain escape was proposed by Lodge and Bates et al.; its key feature is that it includes a broad distribution of exchange rates to account for the polymer's PDI.[23] In contrast to previous TR-SANS studies that considered polydispersity as an explanation for the distribution of rates,[32,56] in Lodge and Bates' model the activation energy for chain escape increases linearly with the number of hydrophobic monomers N and contains an unknown prefactor of order 1[23] that may be related to micelle or chain geometry.[39] Other studies by Lund, Wilner, and Richter[39−41] have shown that the activation energy is proportional to N^{β}, where β is a

DOI: 10.1021/acs.macromol.6b01973
Macromolecules 2017, 50, 2484−2494

scaling exponent that reflects how stretched or collapsed the hydrophobic chain is as it exits the micelle: β varies between 1 (completely stretched, as in Lodge's model[23]) and 2/3 (completely collapsed, as predicted by Halperin and Alexander's scaling theory[38]). Therefore, we use the following relaxation function $K(t,N)$ to model the exchange of BPCs with length N:

$$K(t, N) = \exp\left[-t\frac{6\pi^2 kT}{N^2 b^2 \zeta}\exp(\alpha\chi N^{\beta})\right] \quad (3)$$

where k is Boltzmann's constant, b is the Kuhn length, ζ is the monomeric friction coefficient, χ is the Flory−Huggins interaction parameter, β is the scaling exponent for chain geometry, and α is an unknown prefactor. This equation is identical to Lodge and Bates' relaxation function except that it includes an adjustable β to account for chain stretching or collapse. Following Lodge and Bates' procedure, we integrate this equation over the distribution of chain lengths to obtain the decay in SANS intensity (see Supporting Information).

We attempted to fit this model to our data in two ways: (1) varying β between 2/3 and 1 and using the PDI of 1.15 we obtain for h-PEE using GPC, and (2) varying β in the same way and allowing PDI to take any value ≥1.01. Using method 1, we were able to reject the fit with >99.9% confidence for all six data sets, and β always took a value of 2/3, indicating that allowing a lower effective PDI would improve the fit (see Supporting Information). For method 2, we were able to reject two of the six fits with >99.9% confidence, and all fits yielded both $\beta = 2/3$ and an unrealistically low PDI of 1.01 set by the lower bound in the fitting procedure (in pure BCP micelles, this model matches the PDI from GPC to within 0−0.07[23,40]). Consequently, we conclude that our data are not consistent with the single chain escape mechanism described for pure BCP micelles. More information on our fits to the single chain escape model (including graphs and parameter values) can be found in the Supporting Information.

Having eliminated classical single polymer chain escape, we next apply a simple single-exponential model to our data, representative of a single rate-limiting process as expected if polymer exchange proceeds via fusion or fragmentation. We use basic rate kinetics principles to derive a model for chain exchange, as was done for lipid exchange between vesicles,[28,29] cholesterol exchange between lipid vesicles,[27] and polymer exchange between micelles.[23,32,33,39−42,53,57] We can write the following rate equation for the mixed micelles:

$$\frac{\Delta\rho(t)}{\Delta\rho(0)} = \exp(-k_{ex}t) \quad (4)$$

i.e., that the normalized SLD contrast follows a simple exponential decay with time constant $\tau = k_{ex}^{-1}$.

The data are fit well by this single-exponential model. For completeness, we also tested our data against both a double-exponential and a stretched-exponential model (see Supporting Information). While the fits usually improved somewhat given the extra parameters, a careful statistical analysis of the results (see Supporting Information) clearly shows that our data do not support more complex models than the single exponential, indicating that should there be more than one rate-limiting mechanism at play, all must have the same time constants within the uncertainty of our data. The rate constants obtained from these single-exponential fits are given in Table 2.

Table 2. Rate Constants for Polymer Exchange between Mixed Micelles, Lipid Exchange between Single-Component Vesicles, and 1-Decylpyrene (Hydrophobic Probe) Exchange between Detergent Micelles[a]

temp (°C)	amphiphilic system system	species exchange	k_{ex} (s^{-1})	$t_{ex,1/2}$ (h)
35	BCP + 7 mg/mL OG	BCP	$(1.2 \pm 0.1) \times 10^{-6}$	160 ± 16
	BCP + 8 mg/mL OG	BCP	$(3.6 \pm 0.2) \times 10^{-6}$	53 ± 3
	DMPC vesicles[28]	DMPC	6.2×10^{-5}	3.1
	Triton X-100 micelles	1-decylpyrene	3.4×10^{5}	5.7×10^{-10}
37	POPC vesicles[29]	POPC	2×10^{-6}	90
45	BCP + 7 mg/mL OG	BCP	$(3.6 \pm 0.06) \times 10^{-5}$	5.3 ± 0.08
	BCP + 8 mg/mL OG	BCP	$(5.6 \pm 0.2) \times 10^{-5}$	3.4 ± 0.1
	DMPC vesicles[28]	DMPC	1.7×10^{-4}	1.1
	Triton X-100 micelles	1-decylpyrene	2.4×10^{6}	8.6×10^{-11}
55	BCP + 7 mg/mL OG	BCP	$(7.2 \pm 0.4) \times 10^{-4}$	0.27 ± 0.02
	BCP + 8 mg/mL OG	BCP	$(1.1 \pm 0.2) \times 10^{-3}$	0.18 ± 0.04
	DMPC vesicles[28]	DMPC	4.6×10^{-4}	0.42
	Triton X-100 micelles	1-decylpyrene	1.5×10^{7}	1.3×10^{-11}

[a]For lipid vesicles, flip-flop between the inner and outer leaflets is a second rate-limiting process not observed in micelles. Because rate data were not given at 35 and 55 °C in refs 28 and 47 (or at 45 °C in ref 47), we back-calculated rate constants at these temperatures from the activation energy and rate data given in the references using the Arrhenius equation. Because fusion, the rate-limiting process for the probe exchange in Triton micelles, depends on detergent concentration, the data shown use a value of 18 mg/mL to aid in comparison with the BCP + OG data.

In the two component polymer detergent systems we considered, we would expect three separate time scales: the very long time scale of polymer chain escape, the very short time for detergent chain escape, and a time scale for aggregate level fission/fusion and fragmentation that should vary with polymer:detergent ratio. In the limit of infinite polymer:detergent ratio these last time scales are known to be even slower than polymer chain escape. At the other limit of zero polymer:detergent ratio those time scales are known to be quite fast compared to polymer chain escape: 12 s^{-1} for fragmentation and $(1-2) \times 10^{-6}$ M^{-1} s^{-1} for fusion of Triton X-100 micelles at about 25 °C[47] and about 1/10 that rate for synperonic A7 detergent micelles at similar temperature.[45] Thus, there must be some critical polymer:detergent ratio where the aggregate level processes become faster than single polymer chain escape so that the polymer exchange rate (but not the detergent exchange rate) goes from being dominated by single chain escape kinetics to being dominated by the fission/fusion/fragmentation kinetics.

The polymer exchange rate measured here increases substantially as detergent concentration increases, with the half-life for exchange decreasing about 50% when detergent concentration increases by 1 mg/mL, as shown in Table 2 and Figure 7. This speed-up by many orders of magnitude (compared to kinetics in the absence of OG) coupled with the failure of the polymer escape model to describe the data

DOI: 10.1021/acs.macromol.6b01973
Macromolecules 2017, 50, 2484−2494

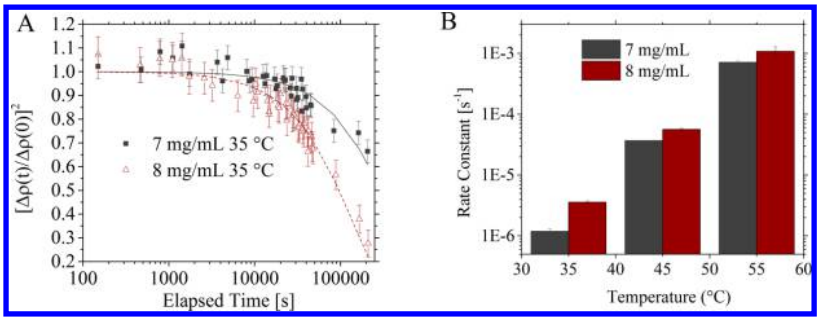

Figure 7. (A) Exchange kinetics are examined as a function of detergent concentration at constant temperature 35 °C. Black data points are for 7 mg/mL OG, and red data points represent 8 mg/mL. Lines represent single-exponential fits to the data. (B) Even a small change in detergent concentration from 7 to 8 mg/mL has an observable effect on the exchange rate constant at all three temperatures examined.

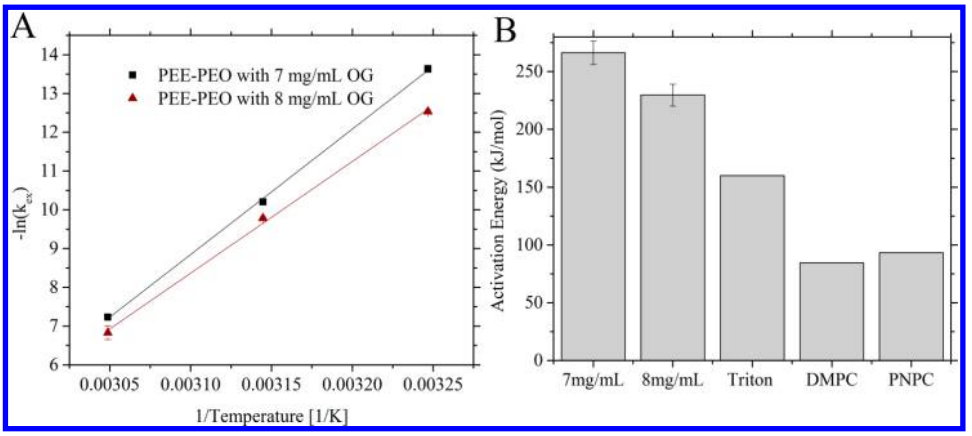

Figure 8. (A) Using the Arrhenius equation (method shown graphically), activation barriers for chain exchange were determined for detergent-solubilized vesicles containing 7 or 8 mg/mL OG. (B) Despite the presence of a moderate amount of detergent, the activation barrier for polymer exchange is substantially larger than for DMPC[28] and PNPC[35] lipid escape or Triton X-100[47] detergent micelle fusion (which was ~10^5 times faster than fission for the Triton micelles[47]).

suggests that at least in this system the critical crossover point between single polymer chain escape and fusion/fission time scales may occur below 7 mg/mL OG. At these relatively low OG concentrations, however (just above the CMC and barely sufficient to completely solubilize the BCP), we would still expect the steric barrier to fusion and fragmentation created by the PEO_{18} corona to remain high and significantly limit the exchange rate in our mixed micelles, as Halperin and Alexander's scaling theory would suggest.[38] Thus, our observation that polymer exchange between mixed micelles remains orders of magnitude slower than detergent micelle fusion and fragmentation is not unreasonable. We also observe that PEE–PEO BCPs exchange between our mixed micelles at a rate comparable to that of DMPC or POPC lipid escape from single-component lipid vesicles (Table 2). Unlike lipids, our BCPs exchange too slowly to quantify in the absence of detergent (see Supporting Information), as expected from the literature.[32,33] Thus, even with the small amount of detergent in our mixed micelles, the apparent cross over from single chain escape to a fusion and fragmentation exchange process leads to polymer exchange rates that are comparable to exchange rates for much smaller amphiphilic molecules.

Having measured the exchange rate constants at three temperatures for samples containing 7 and 8 mg/mL OG and 10 mg/mL PEE–PEO, we estimate the activation barrier to chain exchange using the Arrhenius rate equation:

$$-\ln k_{ex} = \frac{E_A}{RT} - \ln A \qquad (5)$$

where R is the ideal gas constant and A is a process-dependent constant.

The Arrhenius equation yields an activation barrier of 229 ± 10 kJ/mol for 8 mg/mL OG and 267 ± 10 kJ/mol for 7 mg/mL OG (Figure 8). We note that activation barriers for other amphiphilic systems have been estimated using similarly narrow temperature windows: 27–57 °C for DMPC chain escape (84.6 kJ/mol)[28] and 5–25 °C[47] for Triton X-100 micelle fission (110 kJ/mol) and fusion (160 kJ/mol). The larger activation barrier for PEE–PEO exchange between detergent–polymer micelles compared to that of single-component DMPC lipid exchange between lipid vesicles is consistent with the data in Table 2 in showing that the polymer exchange rate is more temperature dependent than the pure DMPC exchange rate. Because of the decrease in the activation barrier as more OG is added (7 vs 8 mg/mL), polymer chain exchange becomes both faster and less temperature dependent at higher OG concentrations. This is again consistent with fusion and/or fragmentation being rate-limiting processes, as a less concentrated polymer corona would result in a lower activation barrier for these mechanisms. In the limit of high detergent:polymer ratio where the activation barrier to PEE–PEO exchange by fusion/fragmentation should become equal to that for OG micelle fusion/fragmentation, we expect that activation barrier could be even smaller than for Triton given that OG has a small sugar headgroup rather than the $PEO_{9.5}$ oligomer of Triton X-100.

After calculating activation energy, we apply the Eyring equations to estimate the enthalpy, entropy, and free energy

DOI: 10.1021/acs.macromol.6b01973
Macromolecules 2017, 50, 2484–2494

changes associated with chain exchange, as has been done for lipid exchange.[35] These values correspond to the barrier between the ground state (a mixed micelle or lipid vesicle) and the transition state. Although our activation energies are estimated from three data points spanning a limited range of temperatures, we believe such analysis can still be informative, particularly when making relative comparisons. In Table 3, we

Table 3. Comparison of Thermodynamic Properties for Chain Exchange between Polymer−Detergent Micelles with Those for Lipid Vesicles and with Those for Hydrophobe Exchange from Detergent Micelles[a]

system studied	E_A (kJ/mol)	$\Delta H^{\ddagger}$ (kJ/mol)	$\Delta S^{\ddagger}$ (kJ/(mol K))	$\Delta G^{\ddagger}$ (kJ/mol)
PEE−PEO + 7 mg/mL OG	266 ± 10	264 ± 10	0.78 ± 0.10	31 ± 20
PEE−PEO + 8 mg/mL OG	230 ± 9	227 ± 9	0.65 ± 0.09	34 ± 18
PNPC	93	91	−0.0015	91
PNPG	93	91	−0.009	94
PNPE	109	106	0.033	96
Triton X-100 (fusion)	160	157	0.17	108
Triton X-100 (fission)	110	108	0.095	79

[a] $\Delta H^{\ddagger}$, $\Delta S^{\ddagger}$, and $\Delta G^{\ddagger}$ values are calculated at 298 K, while E_A values are temperature-independent.

compare these values to those we calculate for the 1-lauroyl-2-[9-(1-pyrenyl)nonanoyl] lipids C_{12}PNPC, C_{12}PNPG, and C_{12}PNPE[35] and Triton X-100 micelles[47] based on literature data.

The thermodynamic results are consistent with the fusion and fragmentation mechanisms seen in some nonionic detergent micelles. The enthalpy barriers to polymer exchange are roughly double those for detergent micelle fission and fusion,[47] consistent with the interpretation that longer PEO chains (present in our mixed micelles) create a greater steric barrier to fragmentation or close contact between micelles (required for fusion)[45] than in Triton X-100 micelles. Increasing the amount of OG in the mixed micelles decreases the enthalpic barrier to exchange, consistent with the corona becoming less dense when more of the micelle surface is occupied by OG rather than BCP.

The entropy changes for the BCP exchange in the polymer/OG systems are also larger in magnitude than for lipid exchange in single-component lipid systems[35] and for hydrophobe exchange in detergent micelles,[47] and the process is entropically favorable for the mixed or detergent micelle cases, whereas it is sometimes unfavorable in the lipid cases. Past studies on polyethylene−PEO BCP micelles have found an entropic gain upon chain exchange which is attributed to chain escape from confinement in the glassy micelle core.[42,43] However, this clearly does not apply in the present case because (1) single chain escape is not consistent with the data and (2) we observe that our polymers are rubbery rather than glassy at room temperature. Probably more relevant to our case is that hydrophobe exchange in Triton X-100 micelles, thought to proceed by fusion and/or fragmentation,[47] is entropically favored (Table 3). Because of the larger entropy change for BCP transfer between mixed micelles compared to lipid escape from single-component lipid vesicles and Triton X-100 micelle fusion, the free energy barrier to polymer exchange between mixed micelles is smaller than for exchange in the other two systems.

While a complete analysis of the various molecular contributions to the enthalpic and entropic components of the transition state are beyond the scope of this work, an interesting potential contribution to the entropic term could originate from stretching of the PEE block in the mixed micelle. Compression or stretching of a polymer chain from its equilibrium size is entropically unfavorable but frequently occurs to minimize the overall free energy of a system,[58−60] and polymer micelles often have their hydrophobic blocks stretched by a factor of 2 or more.[61] Indeed, fission would lead to smaller aggregates which would allow the chains to relax. On the other hand, the total surface area would need to increase which would have both an enthalpic penalty due to the increased hydrophobic/solvent contacts and, according to Rharbi and Winnik,[47] an entropic penalty due to the increased micellar area around which water must form an ordered structure to minimize the disruption to its hydrogen-bonded network. Fusion, on the other hand, would lead to an increase in aggregate diameter by about 25%, further stretching the polymer chains. However, in this case the total surface area would be lowered (less than ideal) which can and will be compensated for by the aggregate taking on a more elongated shape, thus increasing its surface to volume ratio and decreasing the stretching. To the extent that any residual decrease in surface area remains, it would provide another entropically favorable component from the water structure term.

To test whether PEE is stretched or compressed in our mixed micelles, we calculate the degree of stretching defined by Bates et al.[61] as $s = R_{core}/\langle r_0^2\rangle^{1/2}$, where R_{core} is the radius of the micelle's PEE core and $\langle r_0^2\rangle^{1/2}$ is the end-to-end distance for the polymer chain in an ideal random walk configuration. Using a Kuhn length b = 10.5 Å and Kuhn monomer mass M_0 = 230.9 Da for PEE,[62] we calculate that our PEE_{20} chains contain $N_k = N_{EE} \times M_{EE}/M_0$ = 4.85 Kuhn monomers and should have an end-to-end distance $\langle r_0^2\rangle^{1/2} = N_k^{1/2} b$ = 2.31 nm.[59] Using SasView software[52] to obtain a micelle form factor $P(Q)$ from our SANS data, we determined that r_{core} is about 3.7−4.2 nm, indicating that the PEE blocks are stretched by a factor of about 2. Thus, a fission mechanism would provide significant chain relaxation and entropic gain while a fusion mechanism could in principle also provide some chain relaxation if the smallest dimension of the elongated fused aggregate is smaller than the original radius of the micelle. However, whether fusion or fission is the dominant mechanism will depend on the relative strengths of the chain stretching term, the solvent entropic contribution, and the enthalpic penalty, as well as any other contributions to the energetic description of the system and will require a full theoretical and simulation study to sort out.

CONCLUSIONS

The exchange of polymer chains between polymer/detergent micelles is a key step in synthesizing densely packed protein−polymer membranes. Using TR-SANS, partially deuterated polymer, and OG detergent, we directly measure that exchange process. Interestingly, we observe that our data are not consistent with the classic chain extraction mechanism found in polymer micelles and instead suggest the polymer exchanges via the fission/fusion mechanism. The exchange rate increases significantly upon addition of detergent and increase in temperature: the time scale for exchange is too long to measure without OG, even at 50 °C, but is only a matter of

DOI: 10.1021/acs.macromol.6b01973
Macromolecules 2017, 50, 2484−2494

hours with 7 or 8 mg/mL at 45 °C, and less than an hour with 7 or 8 mg/mL OG at 55 °C. Thus, under the right conditions of detergent and temperature, polymer chains can exchange between mixed aggregates even more quickly than has been shown for single-component DMPC and POCP lipid chains.[28,29] Indeed, if polymer exchange proceeds by mixed micelle fusion and/or fission, then we expect that the exchange would become orders of magnitude faster (approaching that of OG micelles) in the limit of high detergent/polymer ratio. Our data are however insufficient to distinguish whether fragmentation or fusion is rate-limiting which is left for future studies. In that vein we note that concentration-dependent studies may yield some insight due to fusion rates being concentration dependent while fission rates are not.[44−48] It is unlikely however to answer the question alone due to a number of experimental challenges including varying OG fraction in the micelle with increasing micelle concentrations arising from the much higher OG CMC.

On the basis of the polymer exchange rates, we calculate that the activation barrier to chain exchange decreases with increasing detergent concentration, making the kinetics faster and less temperature dependent. We also use the Eyring equations[35] to calculate that chain exchange is an entropically favorable process in these mixed systems, both supporting the fission/fusion mechanism[47] and suggesting that polymer chain stretching may play a role in the exchange thermodynamics.[59,61] In combination, these factors lead to the overall barrier to chain exchange between mixed micelles being both substantially smaller and less dependent on chain length than for exchange between single-component polymer or lipid vesicles.

The fact that our data suggest the polymer exchanges via the fission/fusion mechanism in the mixed polymer detergent system is in line with a number of studies on hydrophobic cosurfactant exchange and hydrophobic marker exchange used precisely to study kinetics of micelle fission and fusion.[44−48] Indeed, from the point of view of exchange kinetics these systems should be identical to mixed amphiphile systems containing species with vastly different CMCs (tens of orders of magnitude in our case). However, despite a large body of work on micelle kinetics going back to the 1970s, to our knowledge there remains no theoretical treatment of the kinetics of mixed micelles and in particular the impact of mixed surfactants on the fission/fusion times vs the chain escape rates of the individual components. Single-molecule escape rates from a mixed micelle may or may not change compared to a single-component aggregate, while fission/fusion rates must progress from that of that of the slowest to the fastest component as the micelle composition changes. Thus, we expect that in a mixed micelle whose components have vastly different CMCs, at some critical composition the exchange mechanism for the slower components will transition from single-molecule escape to fission/fusion. We expect that this crossover will be a general phenomenon for mixed micelles, and our data suggest the transition may occur at relatively modest concentrations of the high CMC component. We hope that our work will spur interest from simulators and theorists to better understand this transition.

■ ASSOCIATED CONTENT

Supporting Information

The Supporting Information is available free of charge on the ACS Publications website at DOI: 10.1021/acs.macromol.6b01973.

Supplementary figures, experimental protocols, PEE−PEO synthesis, micelle and vesicle preparation, polymer stock concentration determination, dynamic light scattering, SANS, contrast-matching, statistical analysis, data normalization, comparison of kinetic models (PDF)

■ AUTHOR INFORMATION

Corresponding Authors

*(M.K.) E-mail manish.kumar@psu.edu, Tel (814) 865-7519.
*(P.B.) E-mail pbutler@utk.edu, Tel (301) 975-2028.

ORCID

Kyle J. M. Bishop: 0000-0002-7467-3668
Manish Kumar: 0000-0001-5545-3793

Author Contributions

A.B.S. and P.O.S. contributed equally.

Notes

The authors declare no competing financial interest.

■ ACKNOWLEDGMENTS

This work utilized facilities supported in part by the National Science Foundation (NSF) under Agreement DMR-1508249 and software originally developed as part of the DANSE project funded by the NSF under AgreementDMR-0520547 and currently maintained by NIST, UMD, ORNL, ISIS, ESS, and ILL. Part of the work was also funded by the NSF under Agreement CBET-1512099. Certain commercial equipment, instruments, materials, suppliers, and software are identified in this paper to foster understanding. Such identification does not imply recommendation or endorsement by the National Institute of Standards and Technology, nor does it imply that the materials or equipment identified are necessarily the best available for the purpose.

■ REFERENCES

(1) Samad, A.; Sultana, Y.; Aqil, M. Liposomal drug delivery systems: an update review. *Curr. Drug Delivery* **2007**, *4*, 297.
(2) Howorka, S.; Cheley, S.; Bayley, H. Sequence-specific detection of individual DNA strands using engineered nanopores. *Nat. Biotechnol.* **2001**, *19*, 636.
(3) Shen, Y.-x.; Saboe, P. O.; Sines, I. T.; Erbakan, M.; Kumar, M. Biomimetic membranes: A review. *J. Membr. Sci.* **2014**, *454*, 359.
(4) Bayley, H.; Cremer, P. S. Stochastic sensors inspired by biology. *Nature* **2001**, *413*, 226.
(5) Misra, N.; Martinez, J. A.; Huang, S.-C. J.; Wang, Y.; Stroeve, P.; Grigoropoulos, C. P.; Noy, A. Bioelectronic silicon nanowire devices using functional membrane proteins. *Proc. Natl. Acad. Sci. U. S. A.* **2009**, *106*, 13780.
(6) Noy, A. Bionanoelectronics. *Adv. Mater.* **2011**, *23*, 807.
(7) Fischer, G.; Kosinska-Eriksson, U.; Aponte-Santamaría, C.; Palmgren, M.; Geijer, C.; Hedfalk, K.; Hohmann, S.; De Groot, B. L.; Neutze, R.; Lindkvist-Petersson, K. Crystal structure of a yeast aquaporin at 1.15 Å reveals a novel gating mechanism. *PLoS Biol.* **2009**, *7*, e1000130.
(8) Kumar, M.; Grzelakowski, M.; Zilles, J.; Clark, M.; Meier, W. Highly permeable polymeric membranes based on the incorporation of the functional water channel protein Aquaporin Z. *Proc. Natl. Acad. Sci. U. S. A.* **2007**, *104*, 20719.
(9) Mecke, A.; Dittrich, C.; Meier, W. Biomimetic membranes designed from amphiphilic block copolymers. *Soft Matter* **2006**, *2*, 751.
(10) Selinsky, B. S. *Membrane Protein Protocols: Expression, Purification, and Characterization*; Springer Science & Business Media: 2003; Vol. *228*.

DOI: 10.1021/acs.macromol.6b01973
Macromolecules 2017, 50, 2484−2494

(11) Nardin, C.; Widmer, J.; Winterhalter, M.; Meier, W. Amphiphilic block copolymer nanocontainers as bioreactors. *Eur. Phys. J. E: Soft Matter Biol. Phys.* **2001**, *4*, 403.
(12) Ho, D.; Chu, B.; Lee, H.; Montemagno, C. D. Protein-driven energy transduction across polymeric biomembranes. *Nanotechnology* **2004**, *15*, 1084.
(13) Stoenescu, R.; Graff, A.; Meier, W. Asymmetric ABC-Triblock Copolymer Membranes Induce a Directed Insertion of Membrane Proteins. *Macromol. Biosci.* **2004**, *4*, 930.
(14) Wong, D.; Jeon, T.-J.; Schmidt, J. Single molecule measurements of channel proteins incorporated into biomimetic polymer membranes. *Nanotechnology* **2006**, *17*, 3710.
(15) Kumar, M.; Habel, J. E.; Shen, Y.-x.; Meier, W. P.; Walz, T. High-density reconstitution of functional water channels into vesicular and planar block copolymer membranes. *J. Am. Chem. Soc.* **2012**, *134*, 18631.
(16) Graff, A.; Fraysse-Ailhas, C.; Palivan, C. G.; Grzelakowski, M.; Friedrich, T.; Vebert, C.; Gescheidt, G.; Meier, W. Amphiphilic Copolymer Membranes Promote NADH: Ubiquinone Oxidoreductase Activity: Towards an Electron-Transfer Nanodevice. *Macromol. Chem. Phys.* **2010**, *211*, 229.
(17) Hua, D.; Kuang, L.; Liang, H. Self-directed reconstitution of proteorhodopsin with amphiphilic block copolymers induces the formation of hierarchically ordered proteopolymer membrane arrays. *J. Am. Chem. Soc.* **2011**, *133*, 2354.
(18) Itel, F.; Najer, A.; Palivan, C. G.; Meier, W. Dynamics of membrane proteins within synthetic polymer membranes with large hydrophobic mismatch. *Nano Lett.* **2015**, *15*, 3871.
(19) Morton, D.; Mortezaei, S.; Yemenicioglu, S.; Isaacman, M. J.; Nova, I. C.; Gundlach, J. H.; Theogarajan, L. Tailored polymeric membranes for Mycobacterium smegmatis porin A (MspA) based biosensors. *J. Mater. Chem. B* **2015**, *3*, 5080.
(20) Discher, B. M.; Won, Y.-Y.; Ege, D. S.; Lee, J. C.; Bates, F. S.; Discher, D. E.; Hammer, D. A. Polymersomes: tough vesicles made from diblock copolymers. *Science* **1999**, *284*, 1143.
(21) Grit, M.; Crommelin, D. J. Chemical stability of liposomes: implications for their physical stability. *Chem. Phys. Lipids* **1993**, *64*, 3.
(22) Discher, D. E.; Eisenberg, A. Polymer vesicles. *Science* **2002**, *297*, 967.
(23) Choi, S.-H.; Lodge, T. P.; Bates, F. S. Mechanism of molecular exchange in diblock copolymer micelles: hypersensitivity to core chain length. *Phys. Rev. Lett.* **2010**, *104*, 047802.
(24) Deng, R.; Liang, F.; Zhou, P.; Zhang, C.; Qu, X.; Wang, Q.; Li, J.; Zhu, J.; Yang, Z. Janus Nanodisc of Diblock Copolymers. *Adv. Mater.* **2014**, *26*, 4469.
(25) Kita-Tokarczyk, K.; Grumelard, J.; Haefele, T.; Meier, W. Block copolymer vesicles—using concepts from polymer chemistry to mimic biomembranes. *Polymer* **2005**, *46*, 3540.
(26) Kumar, M.; Habel, J. E.; Shen, Y.-x.; Meier, W. P.; Walz, T. High-density reconstitution of functional water channels into vesicular and planar block copolymer membranes. *J. Am. Chem. Soc.* **2012**, *134*, 18631.
(27) Garg, S.; Porcar, L.; Woodka, A.; Butler, P.; Perez-Salas, U. Noninvasive neutron scattering measurements reveal slower cholesterol transport in model lipid membranes. *Biophys. J.* **2011**, *101*, 370.
(28) Nakano, M.; Fukuda, M.; Kudo, T.; Endo, H.; Handa, T. Determination of interbilayer and transbilayer lipid transfers by time-resolved small-angle neutron scattering. *Phys. Rev. Lett.* **2007**, *98*, 238101.
(29) Nakano, M.; Fukuda, M.; Kudo, T.; Matsuzaki, N.; Azuma, T.; Sekine, K.; Endo, H.; Handa, T. Flip-flop of phospholipids in vesicles: kinetic analysis with time-resolved small-angle neutron scattering. *J. Phys. Chem. B* **2009**, *113*, 6745.
(30) Frindi, M.; Michels, B.; Zana, R. Ultrasonic absorption studies of surfactant exchange between micelles and bulk phase in aqueous micellar solutions of nonionic surfactants with a short alkyl chain. 3. Surfactants with a sugar head group. *J. Phys. Chem.* **1992**, *96*, 8137.
(31) Aoudia, M.; Zana, R. Aggregation behavior of sugar surfactants in aqueous solutions: effects of temperature and the addition of nonionic polymers. *J. Colloid Interface Sci.* **1998**, *206*, 158.
(32) Lund, R.; Willner, L.; Richter, D.; Dormidontova, E. E. Equilibrium chain exchange kinetics of diblock copolymer micelles: Tuning and logarithmic relaxation. *Macromolecules* **2006**, *39*, 4566.
(33) Won, Y.-Y.; Davis, H. T.; Bates, F. S. Molecular exchange in PEO-PB micelles in water. *Macromolecules* **2003**, *36*, 953.
(34) Pedersen, J. S.; Hamley, I. W.; Ryu, C. Y.; Lodge, T. P. Contrast variation small-angle neutron scattering study of the structure of block copolymer micelles in a slightly selective solvent at semidilute concentrations. *Macromolecules* **2000**, *33*, 542.
(35) Homan, R.; Pownall, H. J. Transbilayer diffusion of phospholipids: dependence on headgroup structure and acyl chain length. *Biochim. Biophys. Acta, Biomembr.* **1988**, *938*, 155.
(36) Aniansson, E.; Wall, S. N. Kinetics of step-wise micelle association. *J. Phys. Chem.* **1974**, *78*, 1024.
(37) Kahlweit, M. Kinetics of formation of association colloids. *J. Colloid Interface Sci.* **1982**, *90*, 92.
(38) Halperin, A.; Alexander, S. Polymeric micelles: their relaxation kinetics. *Macromolecules* **1989**, *22*, 2403.
(39) Lund, R.; Willner, L.; Stellbrink, J.; Lindner, P.; Richter, D. Erratum: Logarithmic Chain-Exchange Kinetics of Diblock Copolymer Micelles. *Phys. Rev. Lett.* **2010**, *104*, 049902.
(40) Lund, R.; Willner, L.; Pipich, V.; Grillo, I.; Lindner, P.; Colmenero, J.; Richter, D. Equilibrium chain exchange kinetics of diblock copolymer micelles: Effect of morphology. *Macromolecules* **2011**, *44*, 6145.
(41) Lund, R.; Willner, L.; Richter, D. In *Controlled Polymerization and Polymeric Structures*; Springer: 2013; p 51.
(42) Zinn, T.; Willner, L.; Pipich, V.; Richter, D.; Lund, R. Effect of Core Crystallization and Conformational Entropy on the Molecular Exchange Kinetics of Polymeric Micelles. *ACS Macro Lett.* **2015**, *4*, 651.
(43) Zinn, T.; Willner, L.; Pipich, V.; Richter, D.; Lund, R. Molecular Exchange Kinetics of Micelles: Corona Chain Length Dependence. *ACS Macro Lett.* **2016**, *5*, 884.
(44) Rharbi, Y. Fusion and fragmentation dynamics at equilibrium in triblock copolymer micelles. *Macromolecules* **2012**, *45*, 9823.
(45) Rharbi, Y.; Bechthold, N.; Landfester, K.; Salzman, A.; Winnik, M. A. Solute exchange in synperonic surfactant micelles. *Langmuir* **2003**, *19*, 10.
(46) Rharbi, Y.; Chen, L.; Winnik, M. A. Exchange mechanisms for sodium dodecyl sulfate micelles: high salt concentration. *J. Am. Chem. Soc.* **2004**, *126*, 6025.
(47) Rharbi, Y.; Li, M.; Winnik, M. A.; Hahn, K. G. Temperature dependence of fusion and fragmentation kinetics of Triton X-100 micelles. *J. Am. Chem. Soc.* **2000**, *122*, 6242.
(48) Rharbi, Y.; Winnik, M. A.; Hahn, K. G. Kinetics of fusion and fragmentation nonionic micelles: Triton X-100. *Langmuir* **1999**, *15*, 4697.
(49) Glinka, C.; Barker, J.; Hammouda, B.; Krueger, S.; Moyer, J.; Orts, W. The 30 m small-angle neutron scattering instruments at the National Institute of Standards and Technology. *J. Appl. Crystallogr.* **1998**, *31*, 430.
(50) Kline, S. R. Reduction and analysis of SANS and USANS data using IGOR Pro. *J. Appl. Crystallogr.* **2006**, *39*, 895.
(51) Guinier, A.; Fournet, G. *Small Angle Scattering of X-rays*; J. Wiley & Sons: New York, 1955.
(52) Doucet, M.; Alina, G.; King, S.; Butler, P.; Kienzle, P.; Parker, P.; Kyrzywon, J.; Jackson, A.; Richter, T.; Gonzales, M.; Nielsen, T.; Ferraz Leal, R.; Markvardsen, A.; Heenan, R.; Bakker, J. Sasview Version 3.1.1. http://www/sasview.org; DOI: 10.5281/zenodo.21445, 2015.
(53) Choi, S.-H.; Bates, F. S.; Lodge, T. P. Molecular exchange in ordered diblock copolymer micelles. *Macromolecules* **2011**, *44*, 3594.
(54) Willner, L.; Poppe, A.; Allgaier, J.; Monkenbusch, M.; Richter, D. Time-resolved SANS for the determination of unimer exchange kinetics in block copolymer micelles. *Europhys. Lett.* **2001**, *55*, 667.

DOI: 10.1021/acs.macromol.6b01973
Macromolecules 2017, 50, 2484−2494

(55) Jain, S.; Bates, F. S. On the origins of morphological complexity in block copolymer surfactants. *Science* **2003**, *300*, 460.
(56) Lund, R.; Willner, L.; Stellbrink, J.; Lindner, P.; Richter, D. Logarithmic chain-exchange kinetics of diblock copolymer micelles. *Phys. Rev. Lett.* **2006**, *96*, 068302.
(57) Zinn, T.; Willner, L.; Lund, R.; Pipich, V.; Richter, D. Equilibrium exchange kinetics in n-alkyl−PEO polymeric micelles: single exponential relaxation and chain length dependence. *Soft Matter* **2012**, *8*, 623.
(58) Pata, V.; Dan, N. The effect of chain length on protein solubilization in polymer-based vesicles (polymersomes). *Biophys. J.* **2003**, *85*, 2111.
(59) Rubinstein, M.; Colby, R. H. *Polymer Physics*; OUP: Oxford, 2003.
(60) Bermudez, H.; Brannan, A. K.; Hammer, D. A.; Bates, F. S.; Discher, D. E. Molecular weight dependence of polymersome membrane structure, elasticity, and stability. *Macromolecules* **2002**, *35*, 8203.
(61) Won, Y.-Y.; Brannan, A. K.; Davis, H. T.; Bates, F. S. Cryogenic transmission electron microscopy (Cryo-TEM) of micelles and vesicles formed in water by poly (ethylene oxide)-based block copolymers. *J. Phys. Chem. B* **2002**, *106*, 3354.
(62) Fetters, L.; Lohse, D.; Colby, R. In *Physical Properties of Polymers Handbook*; Springer: 2007; p 447.

DOI: 10.1021/acs.macromol.6b01973
Macromolecules 2017, 50, 2484−2494